

1 **Supporting Information**

2 **Antimicrobial activity of thin-film composite membranes**
3 **functionalized with cellulose nanocrystals and silver nanoparticles**
4 **via one-pot deposition and layer-by-layer assembly**

5
6 Jennifer C. Jackson^a, Camilla H. M. Camargos^{b,c}, Caihong Liu^d, Diego S. T. Martinez^e, Amauri
7 J. Paula^{f,g}, Camila A. Rezende^b, Andreia F. Faria^{a*}

8 *^aEngineering School of Sustainable Infrastructure & Environment, Department of Environmental*
9 *Engineering Sciences, University of Florida, Gainesville, FL, 32611-6580, USA*

10 *^bUniversidade Estadual de Campinas (UNICAMP), Instituto de Química, Departamento de Físico-*
11 *Química, P.O. Box 6154, 13083-970, Campinas, São Paulo, Brazil*

12 *^cSchool of Fine Arts, Universidade Federal de Minas Gerais – UFMG, Belo Horizonte, Minas Gerais,*
13 *31270-901, Brazil*

14 *^dKey Laboratory of Eco-environments in Three Gorges Reservoir Region, Ministry of Education, College*
15 *of Environment and Ecology, Chongqing University, Chongqing 400044, China*

16 *^eBrazilian Laboratory of Nanotechnology, National Center for Research in Energy and Materials –*
17 *CNPEM, Campinas, São Paulo, 13083-100, Brazil*

18 *^fIllum School of Science, National Center for Research in Energy and Materials – CNPEM, Campinas,*
19 *São Paulo, 13083-100, Brazil*

20 *^gPhysics Department, Universidade Federal do Ceará, Fortaleza, Ceará, 60455-900, Brazil*

21 **Corresponding Author (E-mail: andreia.faria@essie.ufl.edu, Tel: 352-392-7104)*

22
23 Supporting information contains 16 pages with 2 sections: in the first section the detailed
24 description of the materials and methods utilized in this work is provided; the second section
25 contains the supplementary figures and tables.

26

27 **SECTION 1: ADDITIONAL METHODS**

28 Confocal Microscopy of *E. coli* on Membranes. **Page S3**

29 **SECTION 2: SUPPLEMENTARY FIGURES**

30 **Figure S1.** TEM of CNC and size distribution. **Page S4**

31 **Figure S2.** Schematic of the reverse osmosis filtration system. **Page S5**

32 **Figure S3.** Photographs of pristine and functionalized membranes. **Page S6**

33 **Figure S4.** Cross-sectional TEM of TFC-OP and TFC-LBL membranes. **Page S7**

34 **Figure S5.** FTIR of pristine and functionalized membranes. **Page S8**

35 **Figure S6.** Graph of XPS full survey of pristine and functionalized membranes. **Page S9**

36 **Figure S7.** High-resolution XPS spectra for pristine and functionalized membranes. **Page**

37 **S10**

38 **Table S1.** Summary of XPS peak deconvolution for high-resolution spectra. **Page S11**

39 **Table S2.** Overview of key parameters impacted by different approaches to functionalize
40 membranes with AgNP. **Page S12**

41 **Figure S8.** Fluorescence images of live and dead *E. coli* cells on the pristine and
42 functionalized membranes. **Page S13**

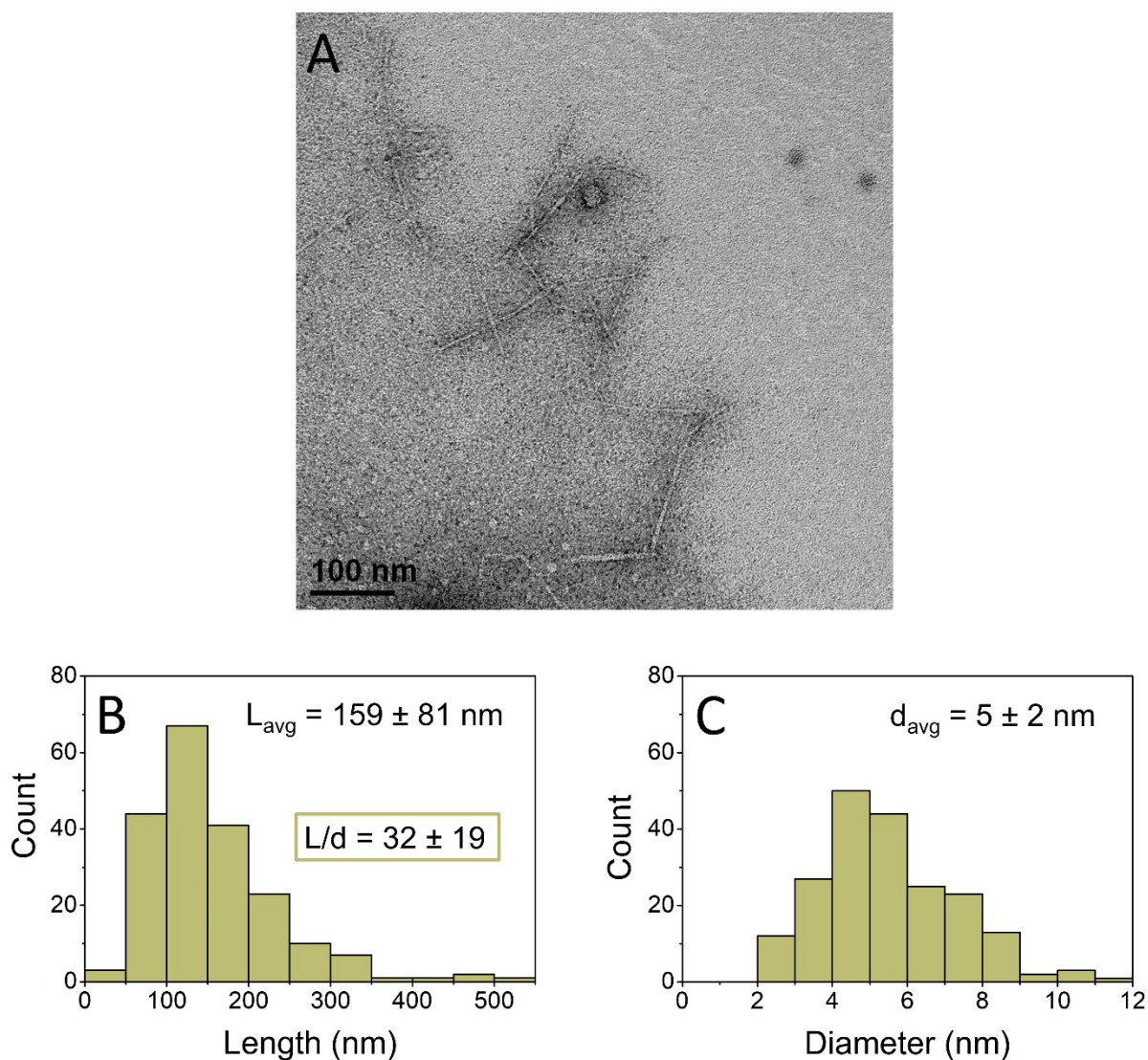
43 **Table S3.** Counts of live/dead cells from fluorescence imaging. **Page S14**

44 **References.** **Page S15**

45 **SECTION 1: ADDITIONAL METHODS**

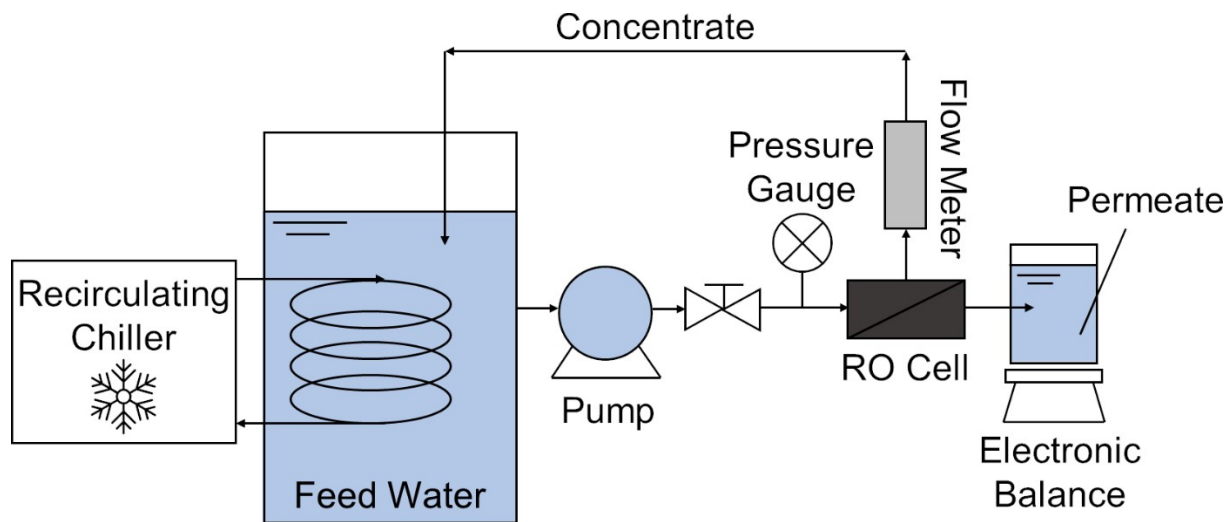
46 **Confocal Microscopy of *E. coli* on Membranes.** Briefly, membrane coupons were placed
47 in PVC holders and contacted with a suspension of *E. coli* at 10^8 CFU/mL for 3 h at room
48 temperature using 3 mL of bacterial suspension per cm^2 of exposed membrane surface. The
49 bacterial suspension was prepared following the methods described in the main manuscript.
50 Membranes were then washed with sterile saline to remove loosely attached cells and some
51 membrane samples were prepared for fluorescence imaging via confocal microscopy. Following
52 the saline wash, 5 mL of fresh, sterile LB was applied to the membrane surface. The membranes
53 in the PVC holders were incubated overnight in static conditions at 37°C to encourage the growth
54 of the well-attached bacteria on the membrane surface into a biofilm. After incubation, the LB was
55 discarded, and the membranes were stained with SYTO 9 to label live cells and propidium iodide
56 (PI) to label dead cells. Stained membranes were imaged in a Nikon A1R MP confocal microscope.
57

58 SECTION 2: SUPPLEMENTARY FIGURES



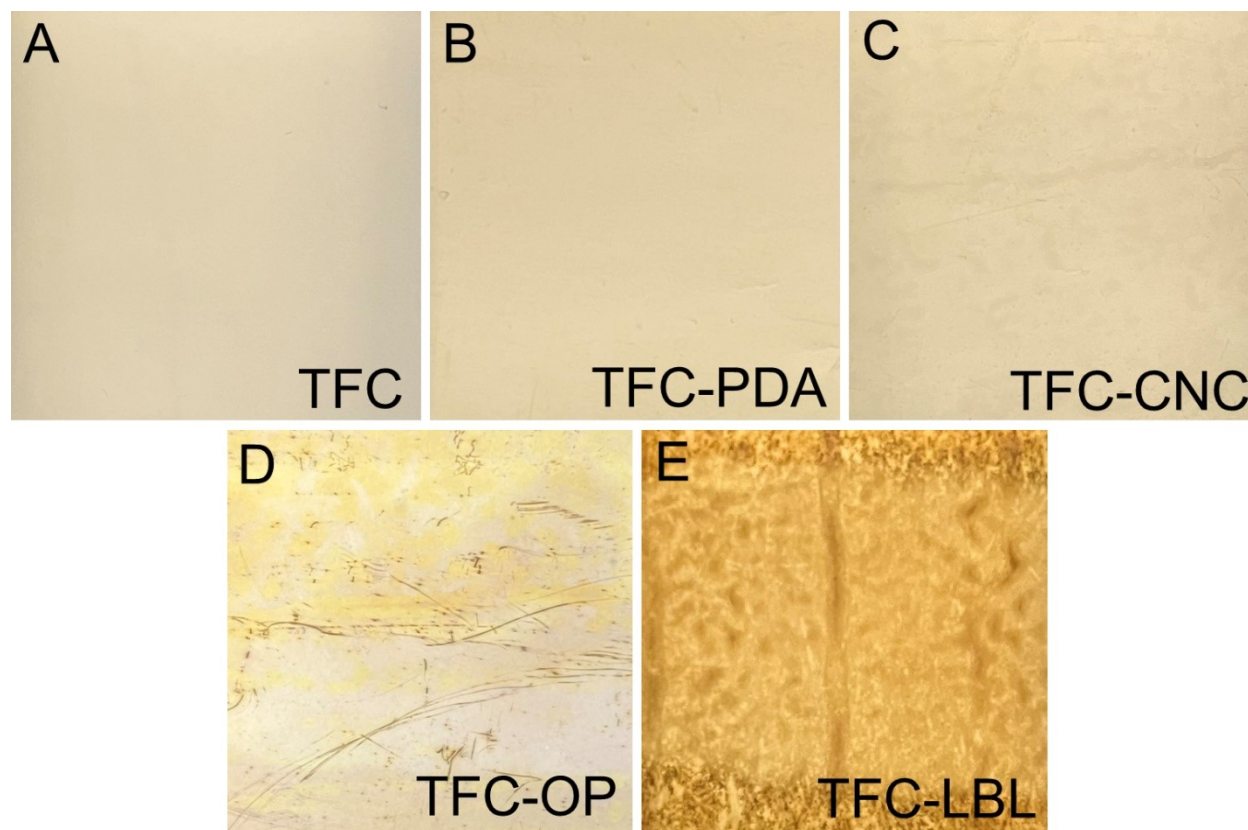
59

60 **Figure S1.** (A) TEM image of cellulose nanocrystals obtained by TEMPO-oxidation followed by
61 sonication of a cellulose-rich substrate isolated from elephant grass leaves. Scale bar: 100 nm. Size
62 distribution histograms of (B) length and (C) diameter measured for 200 nanoparticles in ten
63 different images. The average length and diameter calculated were 159 ± 81 nm and 5 ± 2 nm,
64 respectively. The aspect ratio (length/diameter) was 32 ± 19 .



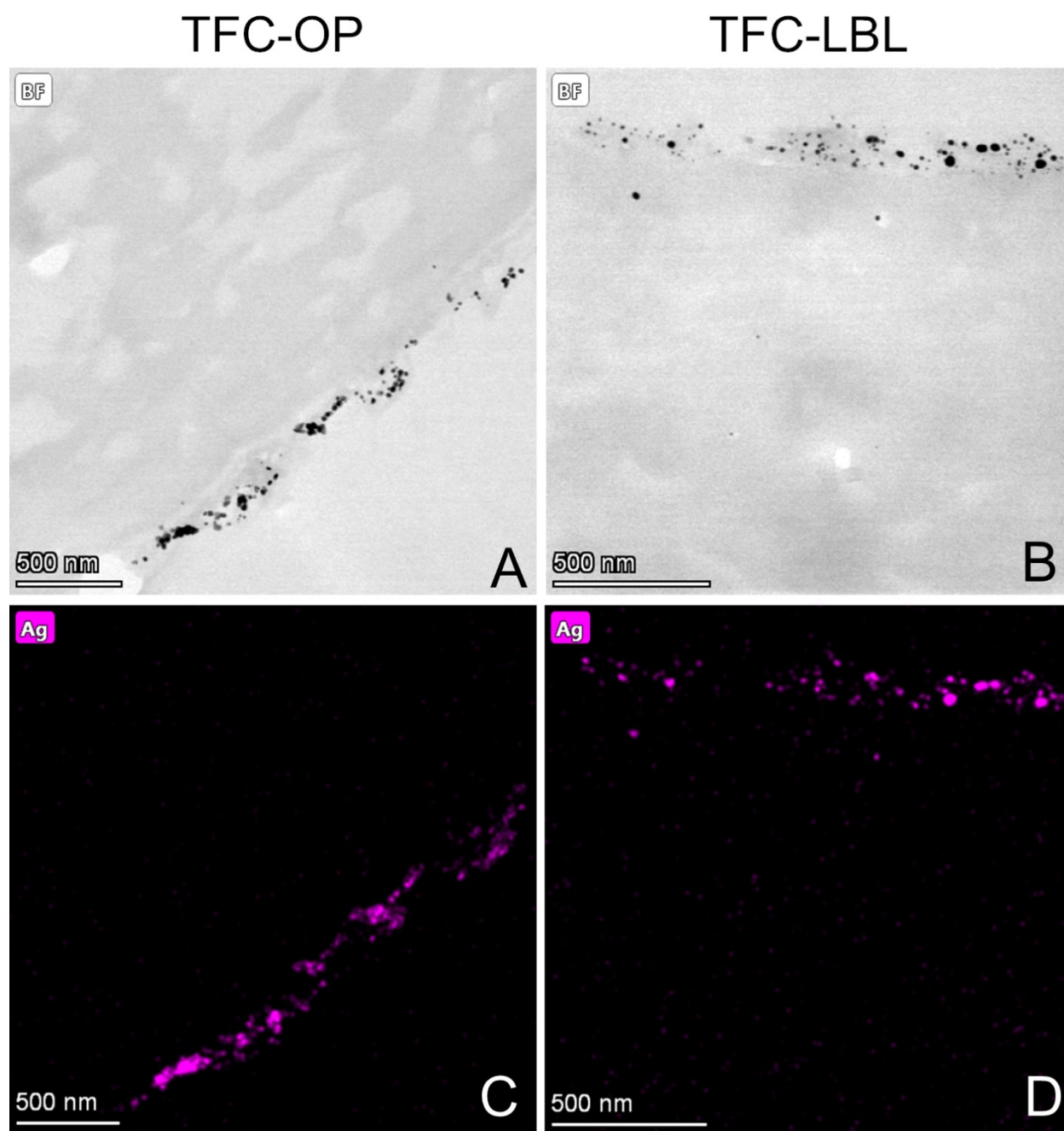
65

66 **Figure S2.** Schematic of the bench-scale reverse osmosis membrane filtration system.



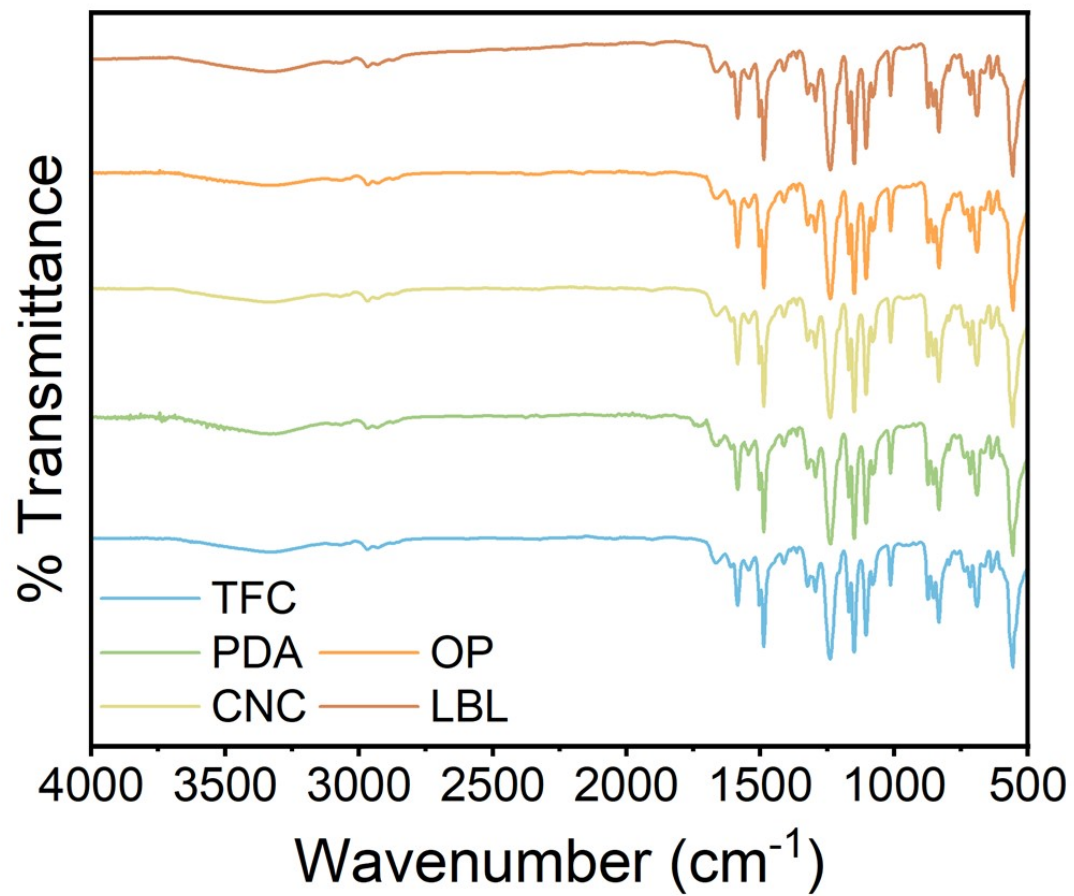
67

68 **Figure S3.** Photographs of the (A) pristine TFC membrane, (B) membrane modified with only
69 PDA (TFC-PDA), (C) membrane modified with CNC using PDA (TFC-CNC), (D) membrane
70 modified using the “one-pot” method to attach CNC/Ag to the membrane surface with PDA (TFC-
71 OP), and (E) membrane modified using the “layer-by-layer” method to attach CNC to the
72 membrane via PDA followed by *in situ* AgNP formation (TFC-LBL).



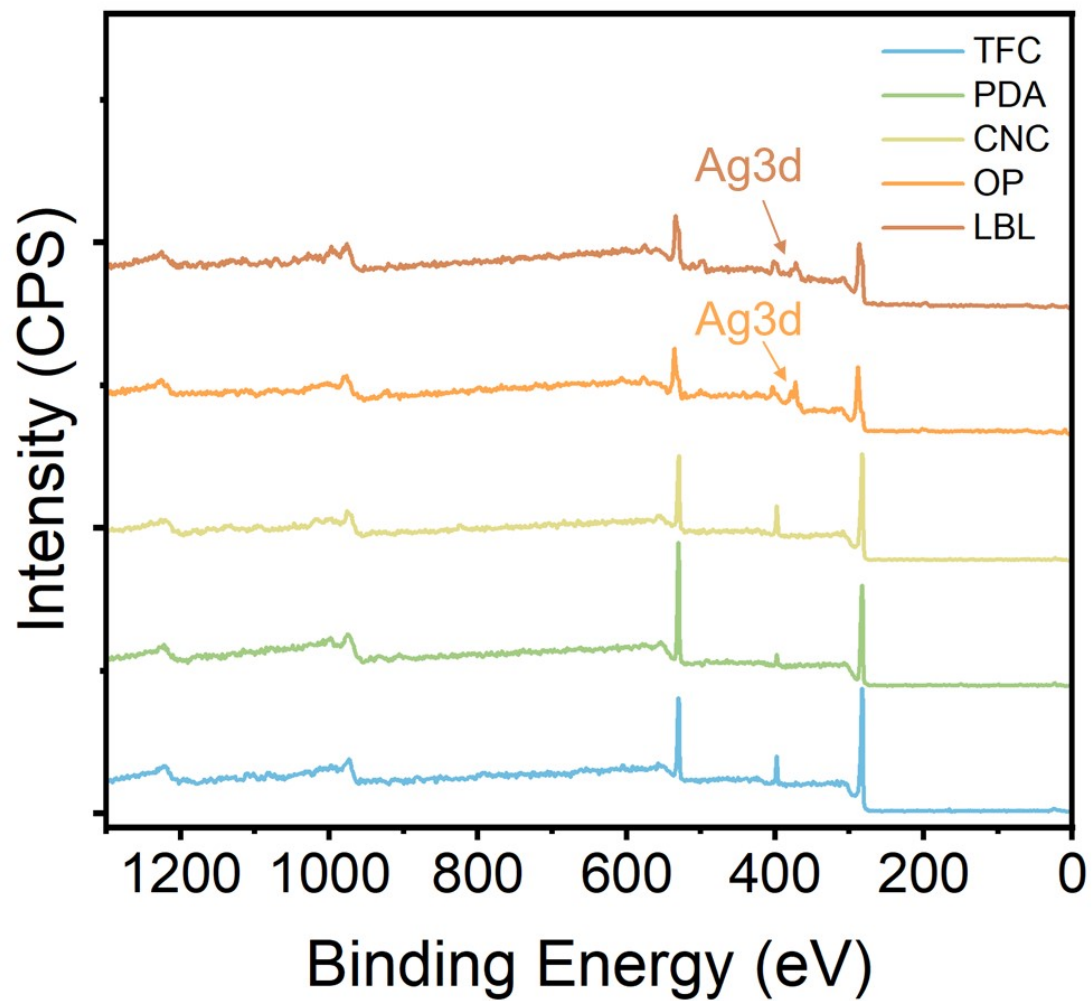
73

74 **Figure S4.** Cross-sectional TEM of the (A) TFC-OP membrane (B) TFC-LBL membrane. In (A)
 75 and (B), the AgNP can be observed as black dots at the membrane surface. EDS analysis was used
 76 to confirm the presence of Ag in these membranes which can be seen indicated by a pink color (C,
 77 D).



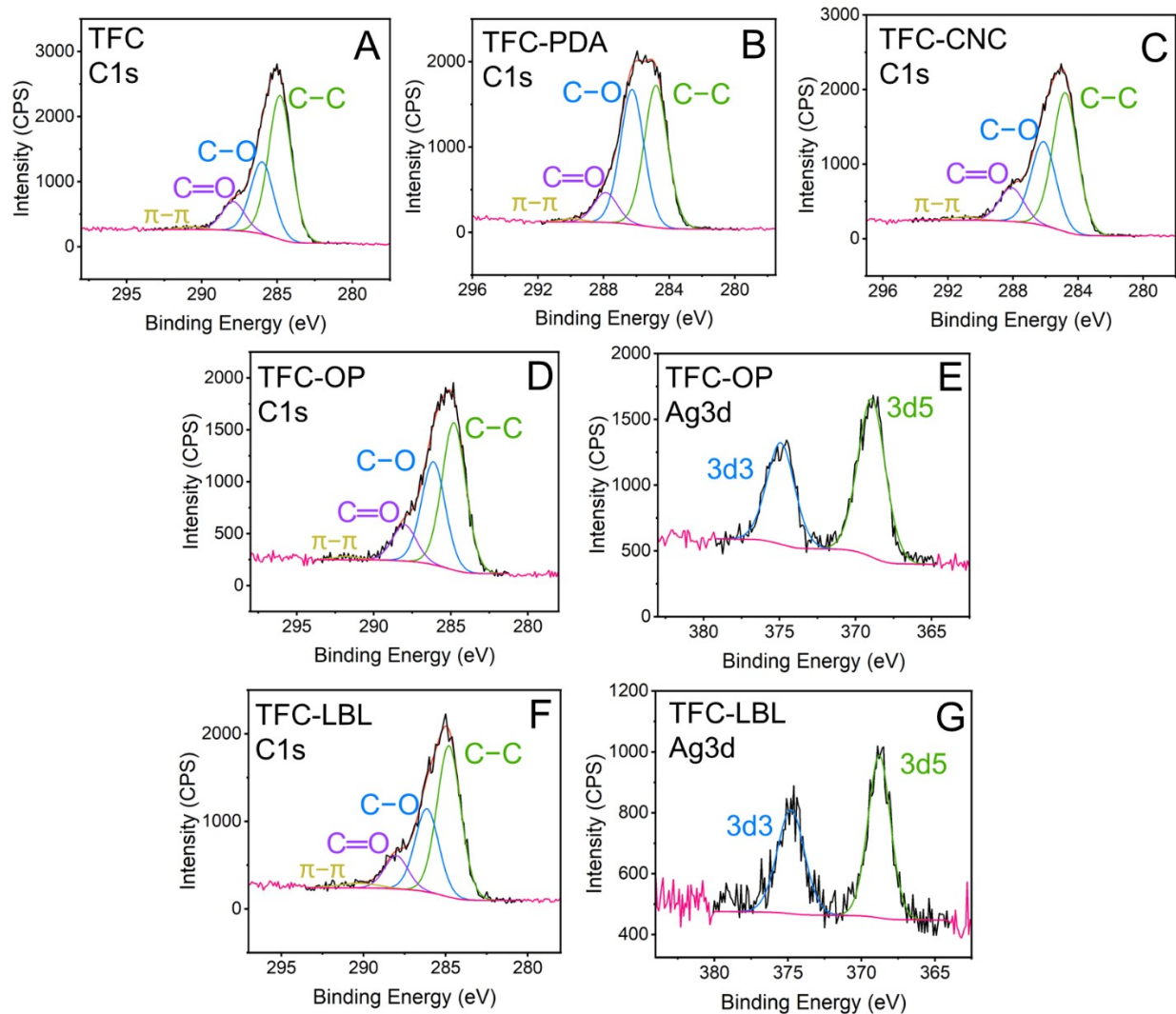
78

79 **Figure S5.** FTIR spectra for the pristine and functionalized membranes.



80

81 **Figure S6.** XPS full survey spectra for the pristine and functionalized membranes.



82

83 **Figure S7.** High-resolution C 1s spectra for the pristine TFC (A), TFC-PDA (B), and TFC-CNC

84 (C) membranes. High-resolution spectra for the TFC-OP membrane for C 1s (D) and Ag 3d (E).

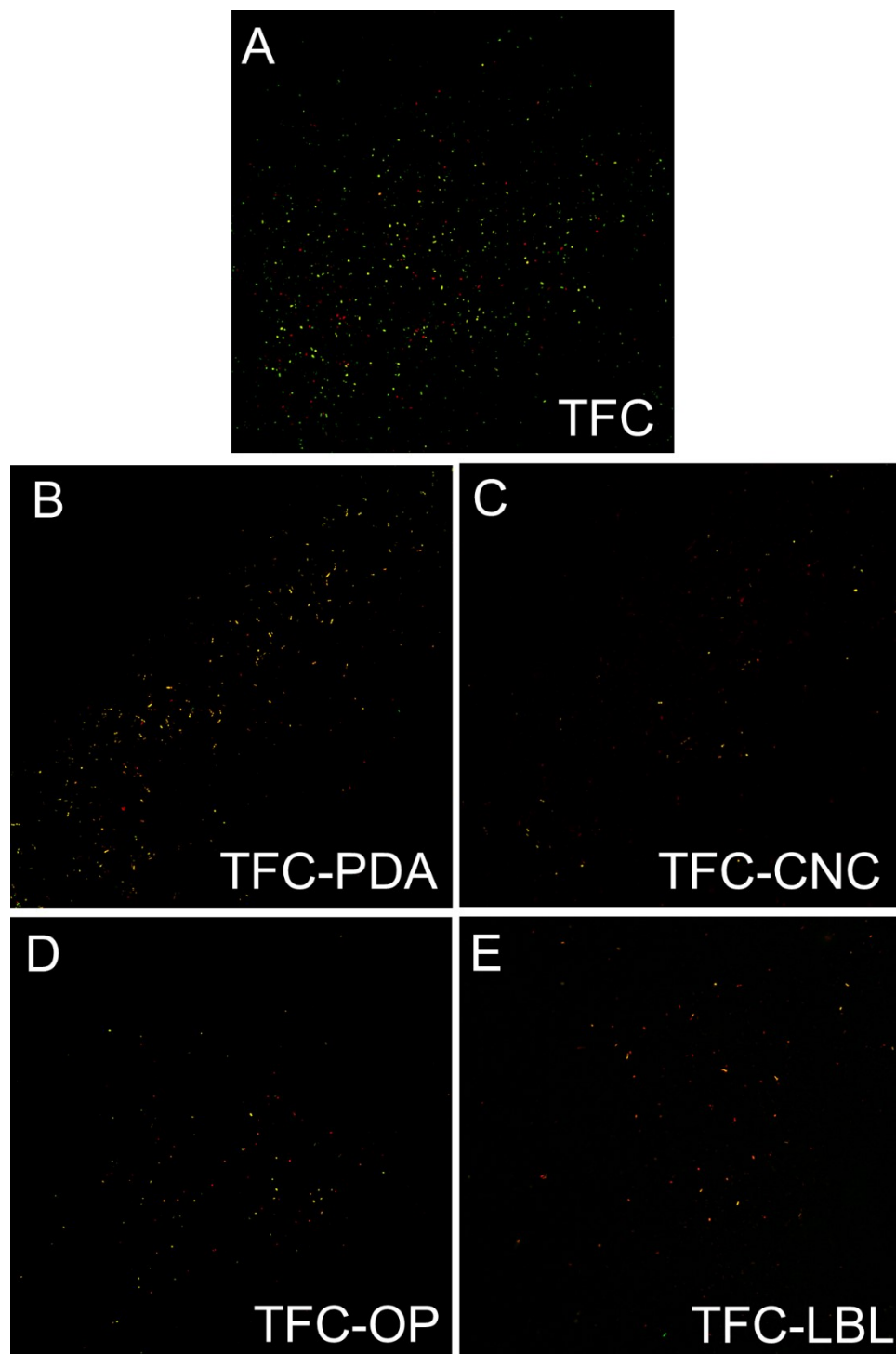
85 High-resolution spectra for the TFC-LBL membrane for C 1s (F) and Ag 3d (G).

86 **Table S1.** Summary of relative peak intensities from XPS analysis of TFC membranes modified
 87 with CNC and AgNP using PDA.

Element	Binding Energy (eV)	Bond	% Area	% Area	% Area	% Area	% Area
			TFC	PDA	CNC	OP	LBL
C 1s	284.8	C–C	58.10	45.78	53.44	50.80	54.86
C 1s	286.0	C–O	29.10	43.51	32.26	35.47	30.19
C 1s	287.9	C=O	11.68	9.66	12.95	12.50	12.05
C 1s	290.7	π – π	1.12	1.05	1.35	1.23	2.90
Ag 3d	368.9	Ag 3d5	N/A	N/A	N/A	60.56	56.54
Ag 3d	374.9	Ag 3d3	N/A	N/A	N/A	39.44	43.46

89 **Table S2.** Overview of key parameters impacted by different approaches to functionalize membranes with AgNP.

Strategy to obtain the silver-containing membrane	Change in water permeability coefficient	Change in salt permeability	Silver loading	Silver leaching rate	Antimicrobial performance	Reference
“One-pot” immobilization of CNC/Ag hybrid	+11%	+89%	1.71 $\mu\text{g cm}^{-2}$	0.027 $\mu\text{g cm}^{-2} \text{ day}^{-1}$	75.7% inactivation of <i>E. coli</i>	This work
“Layer-by-layer” deposition of CNC and <i>in situ</i> nucleation of AgNP	+16%	+494%	3.55 $\mu\text{g cm}^{-2}$	0.091 $\mu\text{g cm}^{-2} \text{ day}^{-1}$	90.1% inactivation of <i>E. coli</i>	This work
AgNP covalently bonded to polyamide active layer	+32%	+2%	15.5 $\mu\text{g cm}^{-2}$	0.1 $\mu\text{g cm}^{-2} \text{ day}^{-1}$	Good inhibition against <i>E. coli</i>	(Yin et al., 2013)
Covalent immobilization of AgNP-decorated silica particles	-3%	+0.2%	0.155 $\mu\text{g cm}^{-2}$	0.0011 $\mu\text{g cm}^{-2} \text{ day}^{-1}$	92.7% (<i>E. coli</i>), 99.5% (<i>P. aeruginosa</i>), 73.3% (<i>S. aureus</i>)	(Park et al., 2015)
<i>In situ</i> generation of AgNP followed by interfacial polymerization	+210%	-7%	14.7 $\mu\text{g cm}^{-2}$	13.1 $\mu\text{g L}^{-1}$ (initial release)	44.4% (<i>E. coli</i>) and 90.1% (<i>B. subtilis</i>)	(Yang et al., 2017)
Covalent immobilization of graphene oxide/AgNP	-10%	+19%	-	-	80% inactivation of <i>P. aeruginosa</i>	(Faria et al., 2017)
Embedding of graphene oxide quantum dot/AgNP via interfacial polymerization	+44%	-0.3%	Up $\sim 4 \mu\text{g mL}^{-1}$ (accumulative release)	$\sim 0.75 \mu\text{g mL}^{-2} \text{ day}^{-1}$	98.6% (<i>E. coli</i>) and 96.5% (<i>S. aureus</i>)	(Yu et al., 2019)
Grafting zwitterionic polymer brushes and AgNP	-31%	+103%	$\sim 7.5 \mu\text{g cm}^{-2}$	$\sim 0.5 \mu\text{g cm}^{-2} \text{ day}^{-1}$	97% inactivation of <i>P. aeruginosa</i>	(Liu et al., 2016)
Addition via interfacial polymerization of tannic acid-functionalized carbon nanotubes embedded with AgNP	+15%	+0.1%	2.29 $\mu\text{g cm}^{-2}$	0.014 $\mu\text{g L}^{-1}$ (initial release)	97.8% inactivation of <i>E. coli</i>	(Zhao et al., 2021)



91

92 **Figure S8.** Confocal images showing *E. coli* cells on the membrane surface following the static
93 biofouling assay. Live cells stained with SYTO 9 are shown in green while dead cells stained with
94 PI are shown in red.

95 **Table S3.** Live and dead cells counted from confocal images taken following the static biofouling
96 assay in darkness.

Sample	Total Cells	Live Cells (%)	Dead Cells (%)
TFC	253	59.7	40.3
TFC-PDA	119	32.8	67.2
TFC-CNC	22	50.0	50.0
TFC-OP	42	28.6	71.4
TFC-LBL	34	26.5	73.5

97

98

99 References

- 100 Faria, A. F., Liu, C., Xie, M., Perreault, F., Nghiem, L. D., Ma, J., & Elimelech, M. (2017).
101 Thin-film composite forward osmosis membranes functionalized with graphene oxide–
102 silver nanocomposites for biofouling control. *Journal of Membrane Science*, 525, 146–156.
103 <https://doi.org/10.1016/J.MEMSCI.2016.10.040>
- 104 Liu, C., Faria, A. F., Ma, J., & Elimelech, M. (2016). Mitigation of Biofilm Development on
105 Thin-Film Composite Membranes Functionalized with Zwitterionic Polymers and Silver
106 Nanoparticles. *Environmental Science & Technology*, 51(1), 182–191.
107 <https://doi.org/10.1021/acs.est.6b03795>
- 108 Park, S.-H., Ko, Y.-S., Park, S.-J., Lee, J. S., Cho, J., Baek, K.-Y., Kim, I. T., Woo, K., & Lee,
109 J.-H. (2015). *Immobilization of silver nanoparticle-decorated silica particles on polyamide*
110 *thin film composite membranes for antibacterial properties*.
111 <https://doi.org/10.1016/j.memsci.2015.09.060>
- 112 Yang, Z., Wu, Y., Guo, H., Ma, X.-H., Lin, C.-E., Zhou, Y., Cao, B., Zhu, B.-K., Shih, K., &
113 Tang, Y. (2017). *A novel thin-film nano-templated composite membrane with in situ silver*
114 *nanoparticles loading: Separation performance enhancement and implications*.
115 <https://doi.org/10.1016/j.memsci.2017.09.046>
- 116 Yin, J., Yang, Y., Hu, Z., & Deng, B. (2013). Attachment of silver nanoparticles (AgNPs) onto
117 thin-film composite (TFC) membranes through covalent bonding to reduce membrane
118 biofouling. *Journal of Membrane Science*, 441, 73–82.
119 <https://doi.org/10.1016/J.MEMSCI.2013.03.060>
- 120 Yu, L., Zhou, W., Li, Y., Zhou, Q., Xu, H., Gao, B., & Wang, Z. (2019). Antibacterial Thin-Film
121 Nanocomposite Membranes Incorporated with Graphene Oxide Quantum Dot-Mediated

122 Silver Nanoparticles for Reverse Osmosis Application. *ACS Sustainable Chemistry and*
123 *Engineering*, 7(9), 8724–8734. <https://doi.org/10.1021/acssuschemeng.9b00598>
124 Zhao, A., Zhang, N., Li, Q., Zhou, L., Deng, H., Li, Z., Wang, Y., Lv, E., Li, Z., Qiao, M., &
125 Wang, J. (2021). Incorporation of Silver-Embedded Carbon Nanotubes Coated with Tannic
126 Acid into Polyamide Reverse Osmosis Membranes toward High Permeability, Antifouling,
127 and Antibacterial Properties. *ACS Sustainable Chemistry and Engineering*, 9(34), 11388–
128 11402. <https://doi.org/10.1021/acssuschemeng.1c03313>
129